Check for updates

# PCCP

## Accepted Manuscript

Volume 18 | Number 1 | 7 January 2016 | Pages 1–636

# PCCP

Physical Chemistry Chemical Physics
www.rsc.org/pccp

ISSN 1463-9076

PERSPECTIVE
Darya Radziuk and Helmuth Möhwald
Ultrasonically treated liquid interfaces for progress in cleaning and separation processes

175 YEARS

ROYAL SOCIETY OF CHEMISTRY

rsc.li/pccp

# Surface Aging Investigation by Means of AFM-Based Methodology and the Evolution of Conservative Nanoscale Interactions

Matteo Chiesa*, Chia-Yun Lai

Laboratory for Energy and Nano-Sciences, Khalifa University of Science and Technology, Abu Dhabi, United Arab Emirates.

The divergence physical properties of surfaces exposed to airborne contaminants in the atmosphere has been widely investigated in the recent year, but agreement regarding the role that airborne hydrocarbon and water contamination have on surface properties evolution remains elusive. Here we investigate the evolution of freshly grown highly oriented pyrolytic graphite (HOPG) surface exposed to a controlled environment solely containing airborne water contamination, i.e. water vapor. Our approach combines standard electromagnetic spectrum-based spectrometry methods and atomic force microscopy based techniques to provide a holistic view of the surface properties. We provide evidence of the role that water adsorption kinetics has on surface properties, interpreting time dependent force-distance profiles and force of adhesion maps directly obtained from the standard observables in a bimodal AFM. To demonstrate the generality of our approach we also apply it to aged calcite surfaces, proving its advantages in providing comprehensive transient characterization of surfaces with sufficient spatial resolution.

**Corresponding Author**

*Email: mchiesa@masdar.ac.ae

## Introduction

The chemical and physical properties of a surface, and hence its reactivity, vary as the surface typically reduces its free energy and tends towards thermodynamic equilibrium with its environment. Adsorption of water[1-2] or other contaminants[1] is the main factor responsible for the evolution of the surface and heavily affects the surface properties. Adsorption of water on carbon surfaces, for example, has been the subject of many experimental studies since the pioneering work on a highly graphitized adsorbents by Kiselev and co-workers in 1968[3]. The topic gains particular practical interest because of its implications for the use of carbon adsorbents in separation processes where the presence of small amounts of water can be of crucial importance[4]. In the recent year this interest seems to have increased and one can find in the literature a consistent amount of investigations that discuss the main contributors responsible for the evolution of freshly grown highly oriented pyrolytic graphite (HOPG) surface towards a more hydrophobic behavior. The fact that the surface turns to a more hydrophobic one is usually regarded as been caused by hydrocarbon contaminants in the air despite not being the solely and mostly present ones[5-7]. Most of the work disregard completely the role that water and possibly its combination with hydrocarbon contaminant plays[8-9] since the role of single or at most few molecular layers of adsorbed water is erroneously believed to lead to a more hydrophilic behavior. This view of water disregards the evidence of ice-like structure of the first adsorbed water layers on hexagonal surface like HOPG under ambient conditions of pressure and temperature. Despite this great body of knowledge in the literature, the theoretical mechanism responsible for temporal variations of surface properties is still not entirely understood and in

particular the role that water plays is almost fully disregarded. This can be partly attributed to the absence of ad-hoc tools and comprehensive experimental methodologies for transient surface characterization, which are needed to shed light on the role that all of contaminants play.

In this study we present an exploratory investigation methodology that relies on a set of different techniques traditionally not used to study the kinetics of adsorption or the change in surface properties. We use Fourier Transform Infrared (FTIR) spectroscopy set up[8, 10-12] to determine adsorption kinetics of water from a controlled environment solely containing airborne water contamination i.e., water vapor and no volatile hydrocarbons. The approach can be extended to adsorption of different species. Specifically, Diffusive Reflectance Infrared Fourier Transform Spectroscopy (DRIFTS) is employed to complement the standard FTIR set-up with a closed reaction chamber that provides the desired controlled environment and allows users to design the type of gas purged into the chamber with defined temperature and relative humidity (RH). The FTIR-DRIFTS provides the necessary capability to investigate the contaminants adsorption kinetics *in situ* ensuring that the observed area is undisturbed due to operational procedures. We also quantify the change of surface properties by means of interpreting the observables obtained from amplitude modulation atomic force microscopy (AM AFM) with a set of newly developed procedure. We reconstruct the nanoscale force profiles between the AFM tip and the sample by utilizing the Sader-Jarvis-Katan formalism for force reconstruction[13-15], and we discuss the evolution of the force versus distance profile with time. The force-distance profiles are complemented by force of adhesion maps[16], directly obtained from the standard observables in a bimodal AFM via non-invasive non-contact mode of operation. We demonstrate the capability of our investigation methodology on graphite and calcite surfaces and we stress the versatility of our approach indicating the advantage that it provides reporting clear evidence of the role that

water adsorption kinetics in addition to the presence of hydrocarbon contaminants has on the evolution of surface properties.

# Materials and methods

## Sample preparation

Highly Ordered Pyrolytic Graphite (HOPG) is chosen as a model sample due to its intrinsic atomic flatness that makes it possible to disregard any morphological effect when studying the evolution of surface properties. We begin by separating adjacent stacked parallel layers of HOPG with traditional scotch tape method creating a pristine surface that is immediately exposed to a controlled $N_2$ environment at 1220 Pa for 24 hours to allow reaching thermodynamic equilibrium (Temperature at 23±2°C and relative humidity (RH) ~55±5%). Similarly, calcite Iceland spar ($CaCO_3$) is morphologically flat. Pristine surfaces are created by mean of a small hammer to mechanically cleave the calcite crystal along the $(101\bar{4})$ cleavage plane. Similar exposure conditions as for graphite were employed.

## Diffuse Reflectance Infrared Fourier Transform Spectroscopy DRIFT-FTIR

A Netzsch drop humidity generator is connected to the HVC-DRP reaction chamber (from Harrick Scientific) mounted in the front sample compartment of a Bruker 80v FTIR spectrometer using a Praying Mantis Diffuse Reflection Accessory. The different instruments are connected with a heat transfer line that allows the whole system to be maintained at constant temperature. Gas cylinders were connected to the reaction chamber to control the purging gas type by use of a mass flow controller. The pristine HOPG surface is placed in the reaction chamber immediately after cleaving (cr. 5 minutes) and reflects the IR beam while being exposed to a predefined

environment designed to study water adsorption and the consequence evolution of the surface. Time 0 refers to the start of a cycle when the sample is mounted in the experimental set up and is exposed to the humid gas (no water adsorbed). Throughout this work we keep the temperature for the transfer lines and the reaction chamber at 42°C. We record the absorbance spectrum in reflective mode by averaging 150 scans with a resolution of 4 $cm^{-1}$. DRIFT records a spectrum every 10 min.

**Force Measurement**

The AFM (Cypher, Asylum Research) was operated in amplitude modulation (AM) mode with standard OLYMPUS cantilevers (AC160TS and AC240TS). The specifications of the cantilever are k (spring constant) $\approx$ 30 N/m, $f_0$ (natural frequency) $\approx$ 300 kHz, and Q $\approx$ 300 for AC160TS and k $\approx$ 2 N/m, $f_0$ (natural frequency) $\approx$ 70 kHz, and Q $\approx$ 100 for AC240TS. Due to this choice of cantilever one can neglect higher eigenmodes and can approximate the motion to the first harmonic[17]. The $f_0$ of the cantilever was obtained by performing a thermal analysis for the free cantilevers at ~30 nm above the sample surface[18]. In order to reconstruct the force ($F_{ts}$), raw amplitude A (A$\equiv$A$_1\equiv$A$_{sp}$) and phase $\varphi$ ($\varphi$=$\varphi_1$) versus separation distance (d) curves were recorded. These curves were converted into Fts versus $d_m$ profiles by exploiting the Sader-Jarvis-Katan (SJK) formalism[14-15]:

$$F_{ts}^*(d) = \frac{2k}{|F_{AD}|} \int_{u=d}^{u=\infty} \left[ \left(1 + \frac{A^{1/2}}{8\sqrt{\pi(u-d)}}\right) \Omega(u) - \frac{A^{3/2}}{\sqrt{2(u-d)}} \frac{d\Omega(u)}{du} \right] du, \qquad (1)$$

The cantilever-surface separation $z_c$ can relate $d_m$, or equivalently d, to the oscillation amplitude

A by $d_{min} \equiv d \approx z_c - A$. $\Omega$ is the normalized frequency shift expressed by:

$$\Omega(d) = \left[ 1 + \frac{A_0}{QA} \cos(\Phi(d)) \right]^{1/2} - 1$$

(2)

where $A_0$ is the free or unperturbed amplitude of oscillation and $\Phi$ is the phase lag relative to the drive force. For convention we assign d = 0 when minima in $F_{ts}$ occurs, i.e., $F_{ts} = F_{AD}$. The robust use of equations (1)-(2) requires that force transitions occur smoothly and that bistability is avoided. This is required to recover the force and energy for the whole range of distances including long range and tip-sample deformation[19]. Smoothness in force transitions is achieved by sufficiently increasing the free amplitude $A_0$ above the critical region of bi-stability[20-21]. For OLYMPUS (AC160TS) cantilevers (Silicon tips), the smooth transition on graphite and calcite samples occurs for values of $A_0$ larger than 20–30 nm when the tip radius R lies in the 5 to 10 nm range and of 35-45 nm for AC240TS[22]. In this work, the tip radius has been monitored by means of in situ method that exploits the concept of critical amplitude $A_c$[22] and with which it has been found that R has always lied in the 5–10 nm range in the experiments.

**Bimodal SASS operation**

The Cypher AFM was operated in bimodal mode by keeping the perturbed amplitude, $A_1$ or $A_{sp}$, of the first mode constant while imaging and allowing the phase shifts of the first and second modes and the amplitude of the second mode respond freely to the tip surface force. Standard OLYMPUS cantilevers (AC240TS) were excited at the first 2 modal resonance frequencies determined by thermal analysis of the cantilevers in the proximity of the sample surface (~50 nm). The effective tip radii were calculated through the critical amplitude $A_c$ method as explained above. The bimodal SASS (Small Amplitude and Small Set-point) mode requires

amplitude $A_1$ to be chosen in the range of the values predicted by the amplitude distance curve illustrated in Fig. 4a and with the requirement to obtain large contrast in the $A_2$ and $\Phi_2$ channels.

Perturbed second mode amplitude $A_2$ was found to in the range ~ 0.01-0.1 nm. The observables in the bimodal SASS images consisted of $A_1$ (amplitude of mode 1), $A_2$ (amplitude of mode 2), $\Phi_1$ (phase of mode 1), $\Phi_2$ (phase of mode 1) see Fig. 4b in addition to topography and mean deflection $z_0$. In our experiments $A_1$ was forced to be a constant ‒ as in standard AM AFM - by the feedback system. Thus, any contrast in $A_1$ is due to error signals induced by the feedback. For the sake of interpretation of the otherwise physically meaningless maps, simple relationships are obtained by numerically integrating the equation of motion[23]. Adhesion maps, i.e. minima in force or force of adhesion $F_{AD}$, in bimodal SASS can be directly obtained from the mean deflection $z_0$ and the spring constant of the first mode $k_{(1)}$ by

$$F_{AD} \approx \bar{F}_{AD} \approx k_{(1)}z_0$$

(3)

Physically the relationship above can be understood by considering that in SASS mode the tip oscillates near the minimum of the tip-surface force profile (i.e. at the bottom f the force-dicatnce "well"). The tip is maintained in a condition that approximates to quasi-static motion and the force reduces to the force at a point by $k_{(1)}z_0$ since amplitudes of oscillation are sub-nm and even sub-angstrom in many cases.

## Results and Discussion

The evolution of the molecular adsorption of water on a HOPG surface when exposed to a controlled $N_2$ environment at temperature of $23\pm2°C$ and relative humidity (RH) ~55±5% is

represented schematically in Fig. 1 a). In Fig. 1b), the green line represents the FTIR molecular fingerprint of a freshly cleaved HOPG sample, whereas the black line refers to a sample exposed to the humidity rich environment for 24 h. Clear peaks between 2850 cm$^{-1}$ and 2950 cm$^{-1}$ are observable in the spectra and are attributed to possible hydrocarbon contamination[24]. It is unclear whether the hydrocarbon signature is due to airborne contaminates[5] or to some residue from the scotch tape cleavage process. The C-H stretching spectra are present throughout the whole experiment and appear as soon as we started recording data, t = 0 h. The peak representing the C-H stretching remains constant over the time of the experiment. If the airborne contamination hypothesis is correct, such contamination must take place immediately after cleaving, since less than 5 min elapse between HOPG exfoliation in ambient and the acquisition of the first spectra in the controlled organic free environment of our DRIFT-FTIR system. Our results confirm qualitatively previous resulted presented by our group[9] collected at different partial pressure. The main variation in the absorbance spectra is in the range between the 3100 and 3600 cm$^{-1}$ where O–H stretching vibration takes place. This indicates water-like layer (band center at 3400 cm$^{-1}$) on the surface as sketched in Fig. 1 a). The integral of the absorbance signal more than doubles in this range over the duration of the experiment. Since the absorbance signal is directly proportional to the concentration of the species (see experimental section), this observation indicates that the main modification of the surface with time is related to the accumulation of water molecules. The FTIR spectra show the evolution of the surface throughout 24 h.
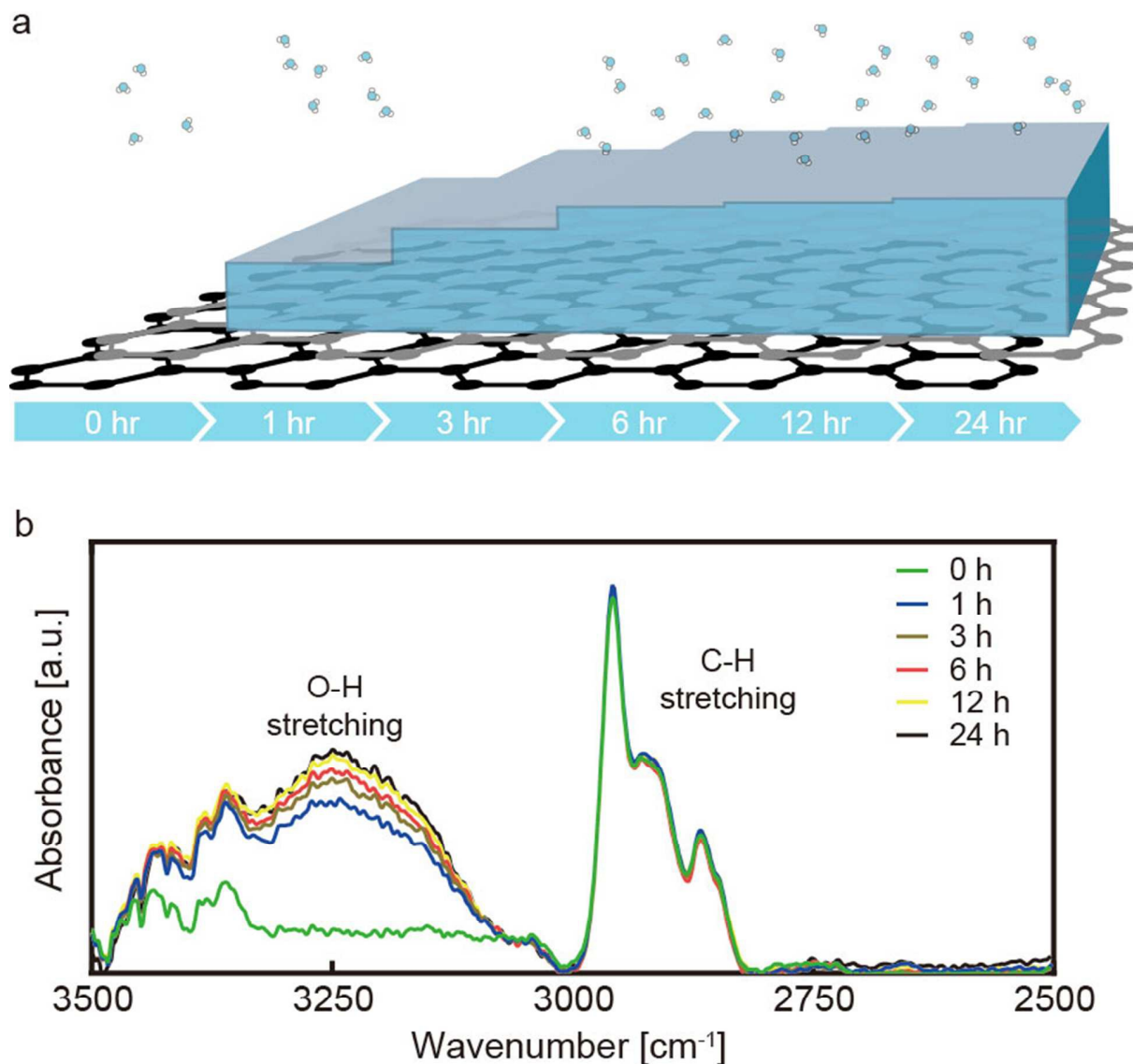
**Figure 1.** a) Graphic representation of the evolution of adsorbed water on a graphitic surface as a function of time b) FTIR absorbance spectra for a freshly cleaved graphite sample (green line), 1 h (blue line), 3 h (brown line), 6 h (red line), 12 h (yellow line) and 24 h (black line) under controlled temperature and RH in a $N_2$ environment at 1220 Pa for 24 hours (Temperature at 23±2°C and relative humidity (RH) ~55±5%). Insets indicate the absorption peaks of hydrocarbon (C-H stretching) and water (ice-like and liquid-like). The main differences between the spectra lie in the region associated to water molecule vibrations (3100–3600 cm−1) while no apparent differences are recorded for the major peaks belonging to C-H stretching between 2850 cm$^{-1}$ and 2950 cm$^{-1}$.
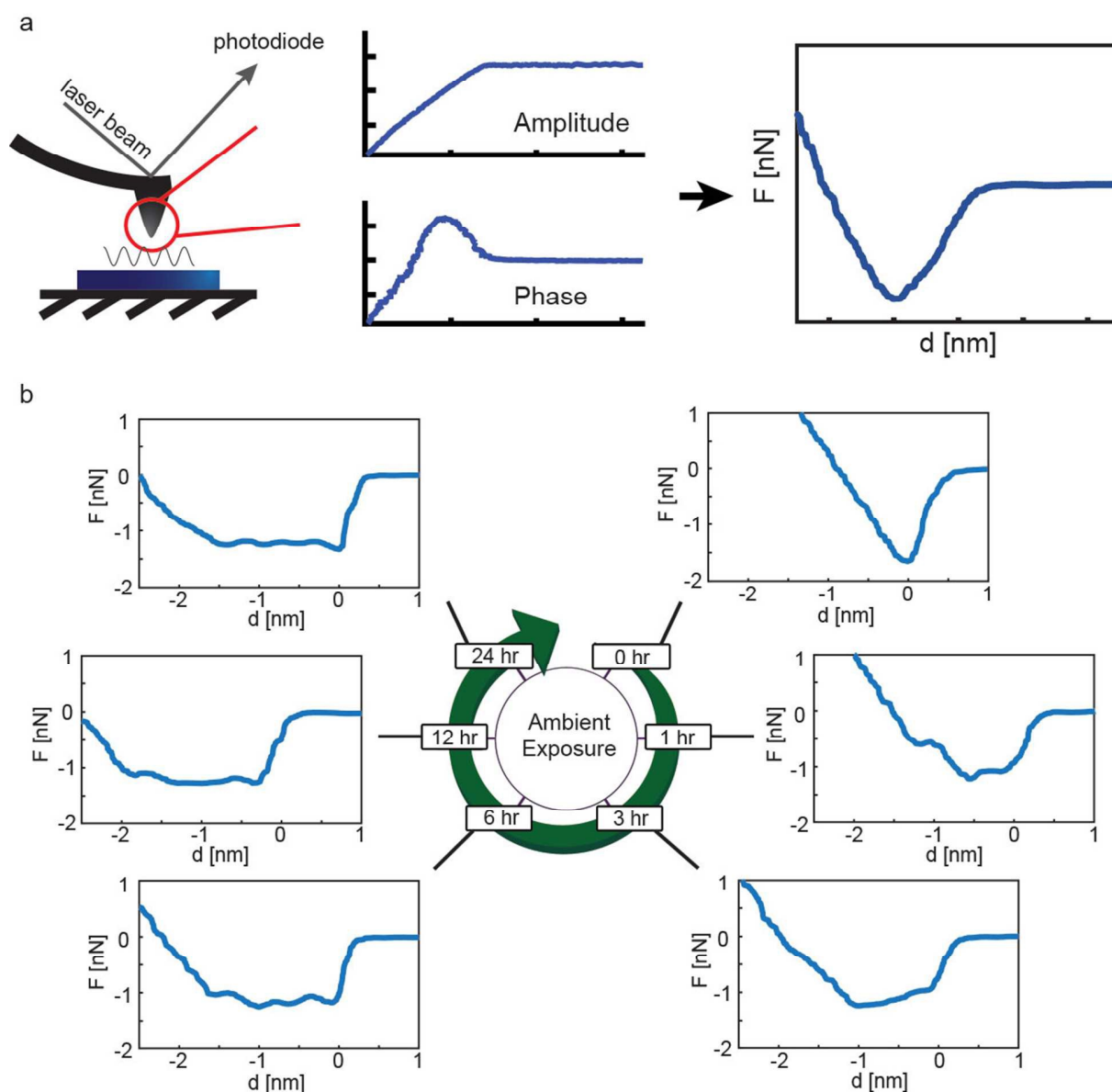
**Figure 2.** a) Schematic of dynamic AM-AFM operation imaging. Oscillation amplitude and tip deflection are tracked via the signal from a laser reflecting from the cantilever onto a photodiode. A sharp (few nm) tip provides molecular scale resolution. Amplitude and Phase-distance profiles are used to reconstruct the conservative fore vs. distance profile. B) Scheme exemplifying the evolution of the conservative force ($F_{TS}$, blue lines) as a function of or d. The data has been acquired just after cleaved graphite 0h, and 1 h, 3 h, 6 h, 12 h and 24 h after keeping the cleaved surface to a controlled environment (Temperature at $23\pm2°C$ and relative humidity (RH) $\sim55\pm5\%$).

The presence of water on the surface is responsible for the evolution of surface properties, which

we observe via the evolution of the interaction between an AFM tip and the HOPG sample

exposed to the controlled environment. AM AFM-based force spectroscopy was carried and the reconstructed conservative force profiles ($F_{TS}$) was reported in Fig 2. The force of adhesion $F_{AD}$, defined as the minimum of the force distance profile, quantifies the strength of tip-surface adherence. The evolution of tip-surface adherence can be observed by looking at the evolution of the $|F_{AD}|$ which starts from a value close to 1.7 nN at time t = 0 h and drops to approximately 1.2 nN after the first hour of exposure. $F_{AD}$ relates to the surface energy $\gamma_{TS}$ as $F_{AD} = 4\pi R \gamma_{TS}$[25] where R is the tip radius; thus a lower absolute value of $F_{AD}$ corresponds to a lower surface free energy of HOPG when the radius is maintained at a constant value (see experimental section). Noted that the AFM tips employed were exposed to the environment long enough to reach thermodynamic equilibrium. That is, as we kept the R unchanged, the variation of the $F_{AD}$ showed in Fig. 2b would only be the result of surface evolution. In addition, in order to rule out the effect of the tip that may lead to the observed outcome, we employed tips with different geometrical parameters as described in the experimental section and both showed the same result. As the surface ages, the $|F_{AD}|$ value stabilizes and maintains a constant value throughout the experiment while the force-distance profile varies diverging from the typical Lennard-Jones type profile. This effect can be monitored by looking at the adhesion energy represented by the area under the $F_{TS}$ curve, which tends to monotonically increase with time. This increase in adhesion energy is compared to the increase of the area under the FTIR spectra and is reported in Fig. 3. The similar trends for the adhesion energy $A_{AD}$ and the $A_{FTIR}$ confirm that the evolution of the profile of the $F_{TS}$ is related to the kinetics of the accumulation of water on the surface. Furthermore, at t > 6 h, the force profile is clearly characterized by a plateau in the vicinity of F $\approx F_{AD}$. We have earlier attempted to relate the extension of this plateau with the increase in height of the adsorbed water layer[26]. The results of Fig. 2 and 3 confirm the capability of AM AFM to

monitor the adsorption of water to HOPG surface over time[27]. It seems that water adsorption

plays a key role in changing the adhesion energy between tip and sample. While we cannot rule

out univocally the role of hydrocarbons they seem to play a secondary role. One key trait of the

AFM spectroscopy technique used here is the fact that one can study adsorption directly on

edges and steps and compare the surface evolution with flat regions that theoretically are thought

of having a different adsorption energy[28]. In the case of HOPG surfaces we are not able to

capture differences in the adsorption mechanism between different regions of the sample because

edges and steps have characteristic dimension comparable to our probe.
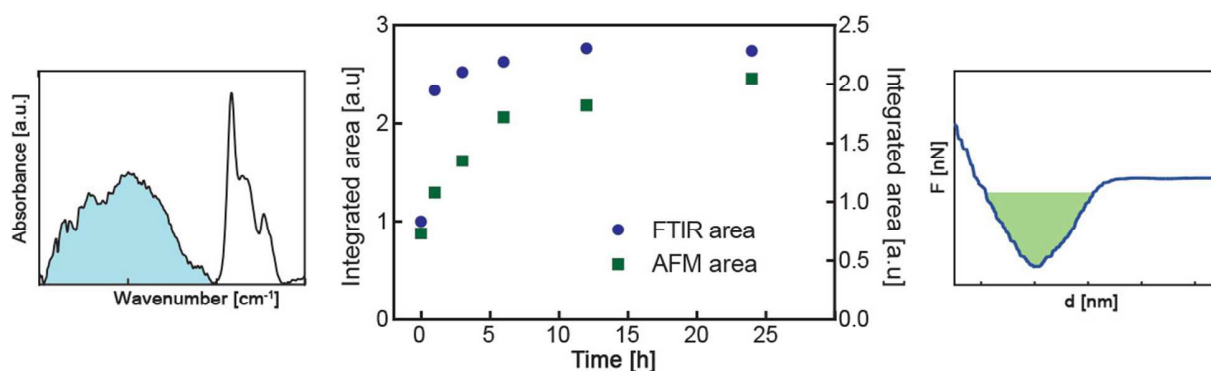


**Figure 3.** Scheme exemplifying how the area under the FTIR spectra (blue area) and conservative force (F, green area) varies as a function of time. Similar trends are recorded hinting to the fact that water adsorption is responsible for the evolution of the force distance curve profile.

In order to confirm the conclusion derived by our spectroscopy experiments and being able to

compare the observations on a larger area we utilize a newly developed technique based on

bimodal SASS. Bimodal SASS mode requires amplitude $A_1$ to be chosen in the range of the

values predicted by the amplitude distance curve illustrated in Fig. S1. The presence of a SASS

region, where the amplitude vs. distance curve changes its monotonically decreasing trend to

slightly increase and subsequently drop in the proximity of the surface, is a necessary

requirement to run the AFM in the SASS mode. The extent of this region is related to the

presence of sufficiently thick water layer as we have explained elsewhere[26]. At time t < 3 h we are not observing the presence of the SASS region and we revert to a different approach while for time t > = 3 h we use the SASS bimodal to directly map force of adhesion $F_{AD}$. By use of Eq. 3 on the obtained raw data we derive $F_{AD}$ maps, which are plotted in Fig. 4 in a similar manner as we did with the force curves. For time t = 0 h and 1 h respectively we were unable to rely on the SASS bimodal operation mode and we revert to the collection of force curves at different data point over an area of 300 nm * 300 nm. Heterogeneity in the histograms is visible by inspection of the histograms for the HOPG sample. The average $<|F_{AD}|>$ is plotted in Fig. 4c.
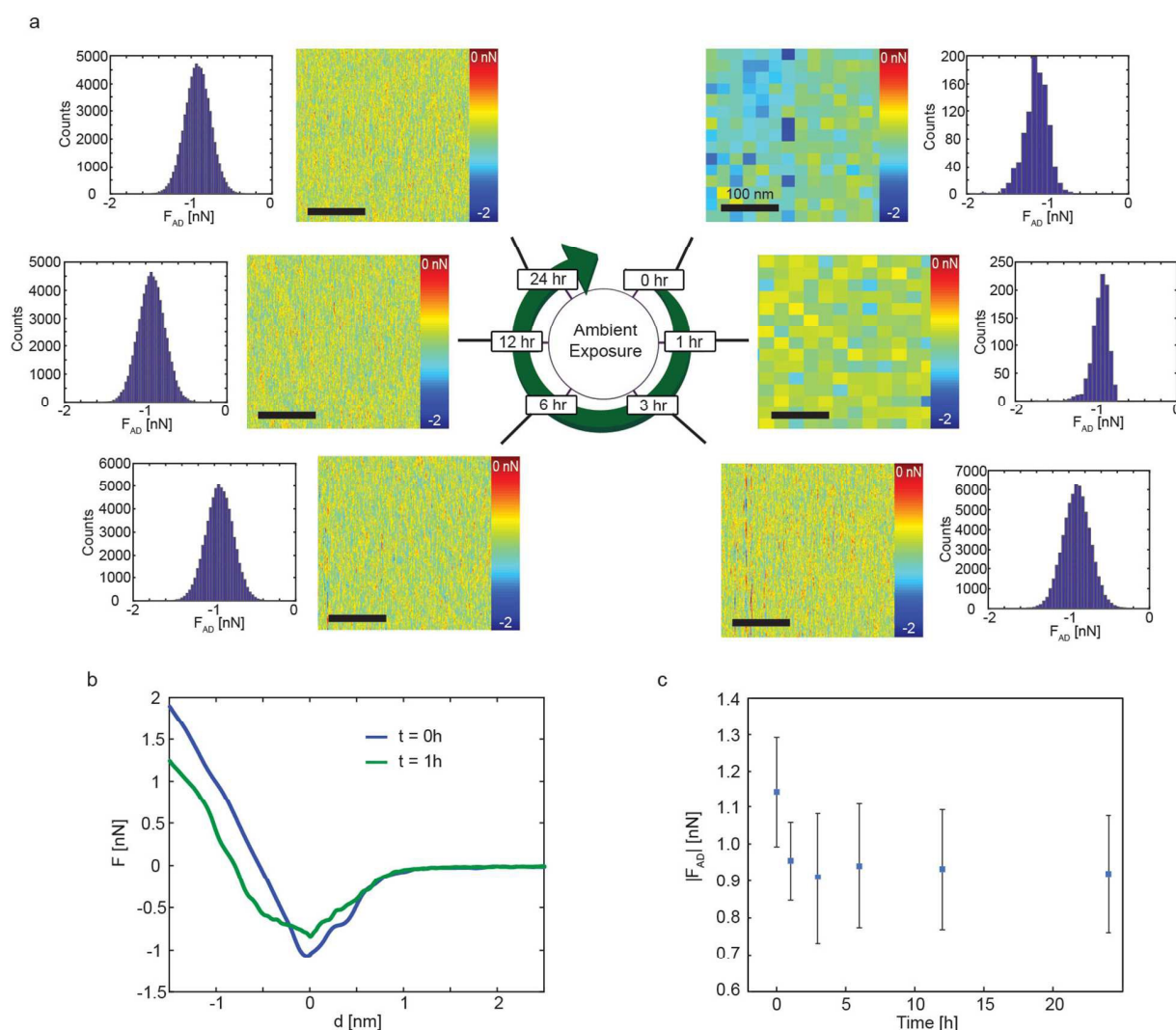
**Figure 4.** a) The graphite force of adhesion, $F_{AD}$ maps are derived for time t= 0 h and 3 h by a series of force-distance profiles collected at different points in the 300nm*300nm area (pixelating images). The $F_{AD}$ maps for later time t > 3h are derived from the observable presented in Fig 4 by employing Eq. 2. The sharp distributions of the force of adhesion value confirm the homogeneity of the surface. b) Characteristic force-distance profile at t= 0h (blue line) and at t= 1h (green line). c) The values for the different timeframes are plotted confirming the trend observed in Fig. 2.

The calcite sample is equally flat as the HOPG, but displays nanoscale chemical heterogeneity, two distinct regions, when the sample is exposed to a water vapor rich environment for a sufficiently long time frame. Fig. 5 illustrates this heterogeneity observed on a calcite surface exposed for 24 h. We combine experiments for which force profiles and force of adhesion

images are acquired to demonstrate the versatility of the AFM based methodology. The two regions on the calcite sample correspond to hydrated and non-hydrated regions on the surface[29]. The values obtained from force profiles were $<F_{AD}> \approx 0.8$ and 0.6 nN for the two phases respectively. These values are in line with the values obtained locally by means of force-distance curves. The sole use of force distance curves would not allow appreciating the spatial growth of the hydrated phase due to the accumulation of atmospheric vapor aqueous with the calcite mineral.
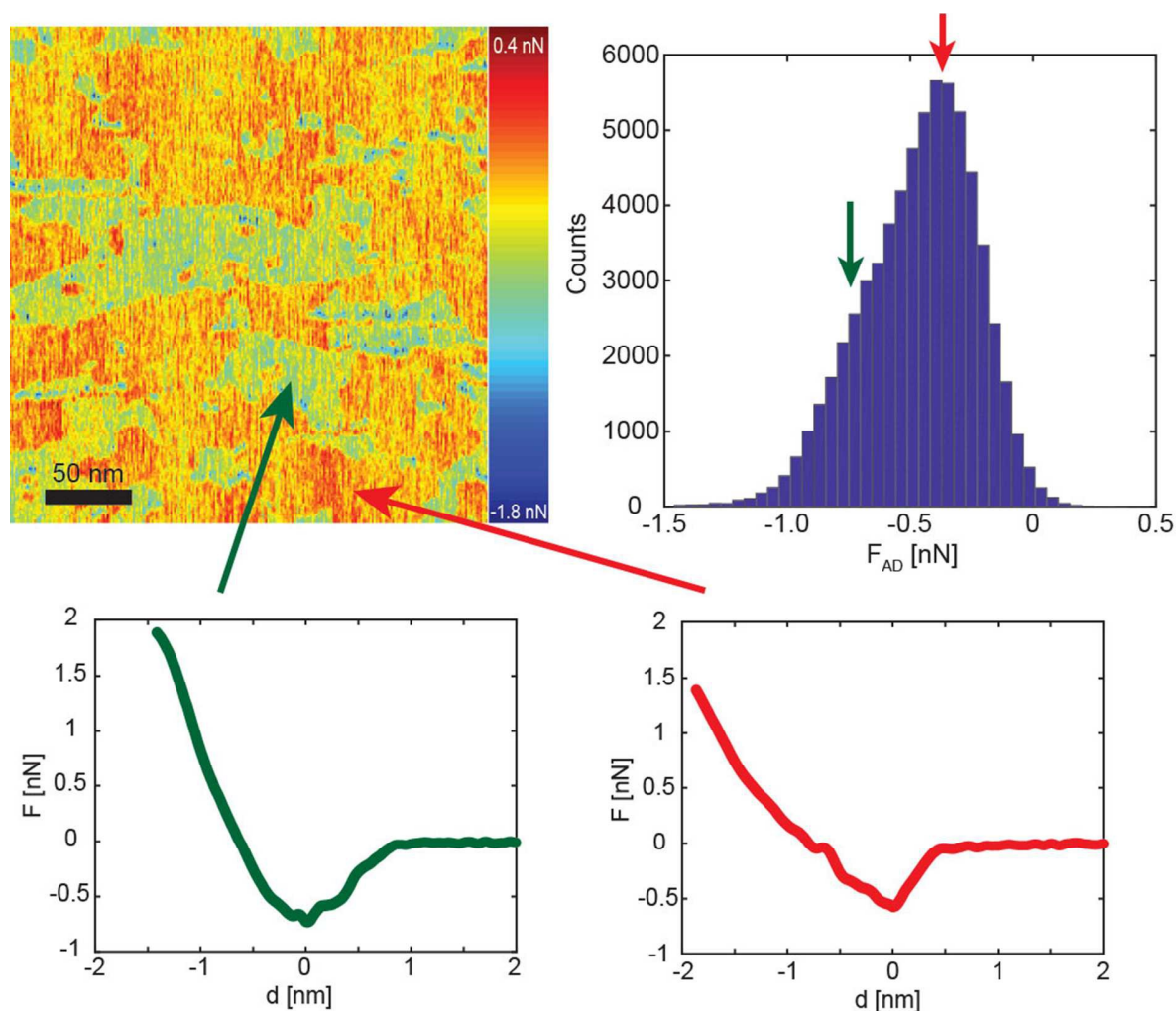


**Figure 5.** Calcite force of adhesion map form a SASS bimodal experiment. The $F_{AD}$ is recorded on a calcite surface kept in a controlled $N_2$ environment at constant temperature and humidity as previously done for calcite (Temperature at 23±2°C and relative humidity (RH) ~55±5%). The bimodal distribution of the $F_{AD}$ map values agrees with local force curves $F_{AD}$.

## Conclusion

In summary, an approach that combines standard electromagnetic-based spectrometry methods and atomic force microscopy based techniques to provide a holistic view of the evolution of surface properties. We demonstrate the robustness of the SASS bimodal AFM operation mode employed to recover the $F_{AD}$ directly from experimental observables while imaging. The values of $F_{AD}$ obtained from the bimodal SASS agree with the observation from experimental force profiles, but provides the capability of investigating the spatial growth of heterogeneities on the surfaces due to contaminants adsorption. These high spatial observations are fundamental in proposing models that describe aging mechanisms. We designed our experiments with the aim of simplifying any surface related morphology aspects that may affect the adsorption process and make the interpretation of the results challenging. Furthermore, our environment was solely rich in water vapor with no other type of contaminants. The approach provides clear evidence of the role that water adsorption kinetics has on surface properties by interpreting time dependent force-distance profiles and force of adhesion maps directly obtained from the standard observables in a bimodal AFM. The generality of our approach is put to test on 2 different surfaces. We acknowledge that more complex systems might lead to models that significantly diverge from the predictions of the expressions for the force employed in this work, but the combinatory work of force spectroscopy and bimodal SASS can help coping with similar effects as it was the case when mapping the $F_{AD}$ of HOPG. We could not operate in SASS regime before sufficient amount of water was accumulated on the surface. An alternative way to do the chemical imaging is to integrate IR spectroscopy with AFM techniques, *i.e.,* nano-IR[30-32], which could simultaneously provide high resolution chemical composition along with sample

topography. On the other hand, we have demonstrated that our approach is general enough that it can be applied to a range of samples.

## Acknowledgements

## References

1.      Balmer, T. E.; Christenson, H. K.; Spencer, N. D.; Heuberger, M., The Effect of Surface Ions on Water Adsorption to Mica†. *Langmuir : the ACS journal of surfaces and colloids* **2007,** *24* (4), 1566-1569.

2.      Beaglehole, D.; Christenson, H., Vapor adsorption on mica and silicon: entropy effects, layering, and surface forces. *The Journal of Physical Chemistry* **1992,** *96* (8), 3395-3403.

3.      Belyakova, L. D.; Kiselev, A. V.; Kovaleva, N. V., Gas-chromotographic determination of isotherms and heats of adsorption of water, benzene and methanol vapours on graphitised carbon black. *Russ. J. Phys. Chem.* **1968,** *42* (9).

4.      Salame, I. I.; Bagreev, A.; Bandosz, T. J., Revisiting the Effect of Surface Chemistry on Adsorption of Water on Activated Carbons. *The Journal of Physical Chemistry B* **1999,** *103* (19), 3877-3884.

5.      Li, Z.; Wang, Y.; Kozbial, A.; Shenoy, G.; Zhou, F.; McGinley, R.; Ireland, P.; Morganstein, B.; Kunkel, A.; Surwade, S. P.; Li, L.; Liu, H., Effect of airborne contaminants on the wettability of supported graphene and graphite. *Nature materials* **2013,** *12*, 925.

6.      Mücksch, C.; Rösch, C.; Müller–Renno, C.; Ziegler, C.; Urbassek, H. M., Consequences of Hydrocarbon Contamination for Wettability and Protein Adsorption on Graphite Surfaces. *The Journal of Physical Chemistry C* **2015,** *119* (22), 12496-12501.

7.      Kozbial, A.; Li, Z.; Sun, J.; Gong, X.; Zhou, F.; Wang, Y.; Xu, H.; Liu, H.; Li, L., Understanding the intrinsic water wettability of graphite. *Carbon* **2014,** *74*, 218-225.

8.      Lai, C.-Y.; Tang, T.-C.; Amadei, C. A.; Marsden, A. J.; Verdaguer, A.; Wilson, N.; Chiesa, M., A nanoscopic approach to studying evolution in graphene wettability. *Carbon* **2014,** *80* (0), 784-792.

9.      Amadei, C. A.; Lai, C.-Y.; Heskes, D.; Chiesa, M., Time dependent wettability of graphite upon ambient exposure: The role of water adsorption. *The Journal of chemical physics* **2014,** *141* (8), 084709.

10.     Danon, A.; Stair, P. C.; Weitz, E., FTIR Study of CO2 Adsorption on Amine-Grafted SBA-15: Elucidation of Adsorbed Species. *The Journal of Physical Chemistry C* **2011,** *115* (23), 11540-11549.

11.     Szanyi, J.; Kwak, J. H.; Zhu, H.; Peden, C. H. F., Characterization of Cu-SSZ-13 NH3 SCR catalysts: an in situ FTIR study. *Physical Chemistry Chemical Physics* **2013,** *15* (7), 2368-2380.

12.     Dong Hwan, S.; Tolou, S.; Chang Kyoung, C.; Seong-Hyuk, L.; Craig, F., Wettability changes of TiO 2 nanotube surfaces. *Nanotechnology* **2011,** *22* (31), 315704.

13.     John, E. S.; Takayuki, U.; Michael, J. H.; Alan, F.; Yoshikazu, N.; Suzanne, P. J., Quantitative force measurements using frequency modulation atomic force microscopy—theoretical foundations. *Nanotechnology* **2005,** *16* (3), S94.

14.     Sader, J. E.; Jarvis, S. P., Accurate formulas for interaction force and energy in frequency modulation force spectroscopy. *Appl. Phys. Lett.* **2004,** *84* (10), 1801-1803.

15.     Katan, A. J.; van Es, M. H.; Oosterkamp, T. H., Quantitative force versus distance measurements in amplitude modulation AFM: a novel force inversion technique. *Nanotechnology* **2009,** *20* (16), 165703.

16.     Herruzo, E. T.; Perrino, A. P.; Garcia, R., Fast nanomechanical spectroscopy of soft matter. *Nat Commun* **2014,** *5*, 3126.

17.     Rodríguez, T. R.; García, R., Tip motion in amplitude modulation (tapping-mode) atomic-force microscopy: Comparison between continuous and point-mass models. *Appl. Phys. Lett.* **2002,** *80* (9), 1646-1648.

18.     Hutter, J. L.; Bechhoefer, J., Calibration of atomic‑force microscope tips. *Review of Scientific Instruments* **1993,** *64* (7), 1868-1873.

19.     Santos, S.; Amadei, C. A.; Verdaguer, A.; Chiesa, M., Size Dependent Transitions in Nanoscale Dissipation. *The Journal of Physical Chemistry C* **2013,** *117* (20), 10615-10622.

20.     Sergio, S.; Victor, B.; Josep, F.; Neil, H. T., Cantilever dynamics in amplitude modulation AFM: continuous and discontinuous transitions. *Journal of Physics D: Applied Physics* **2010,** *43* (27), 275401.

21.     Santos, S.; Barcons, V.; Font, J.; Thomson, N. H., Bi-stability of amplitude modulation AFM in air: deterministic and stochastic outcomes for imaging biomolecular systems. *Nanotechnology* **2010,** *21* (22), 225710.

22.     Santos, S.; Guang, L.; Souier, T.; Gadelrab, K.; Chiesa, M.; Thomson, N. H., A method to provide rapid in situ determination of tip radius in dynamic atomic force microscopy. *Review of Scientific Instruments* **2012,** *83* (4), 043707.

23.     Lai, C.-Y.; Santos, S.; Chiesa, M., Systematic Multidimensional Quantification of Nanoscale Systems From Bimodal Atomic Force Microscopy Data. *ACS nano* **2016,** *10* (6), 6265-6272.

24.     Snyder, R. G.; Hsu, S. L.; Krimm, S., Vibrational spectra in the C ･ H stretching region and the structure of the polymethylene chain. *Spectrochimica Acta Part A: Molecular Spectroscopy* **1978,** *34* (4), 395-406.

25.     Yaminsky, V. V., The hydrophobic force: the constant volume capillary approximation. *Colloids Surf. Physicochem. Eng. Aspects* **1999,** *159* (1), 181-195.

26.     Amadei, C. A.; Santos, S.; Pehkonen, S. O.; Verdaguer, A.; Chiesa, M., Minimal Invasiveness and Spectroscopy-Like Footprints for the Characterization of Heterogeneous Nanoscale Wetting in Ambient Conditions. *The Journal of Physical Chemistry C* **2013,** *117* (40), 20819-20825.

27.     Luna, M.; Colchero, J.; Baró, A. M., Study of Water Droplets and Films on Graphite by Noncontact Scanning Force Microscopy. *The Journal of Physical Chemistry B* **1999,** *103* (44), 9576-9581.

28.     Collignon, B.; Hoang, P. N. M.; Picaud, S.; Rayez, J. C., Ab initio study of the water adsorption on hydroxylated graphite surfaces. *Chem. Phys. Lett.* **2005,** *406* (4–6), 430-435.

29.     Lai, C.-Y.; Cozzolino, M.; Diamanti, M. V.; Al Hassan, S.; Chiesa, M., Underlying Mechanism of Time Dependent Surface Properties of Calcite (CaCO3): A Baseline for Investigations of Reservoirs Wettability. *The Journal of Physical Chemistry C* **2015,** *119* (52), 29038-29043.

30.     Kjoller, K.; Felts, J. R.; Cook, D.; Prater, C. B.; King, W. P., High-sensitivity nanometer-scale infrared spectroscopy using a contact mode microcantilever with an internal resonator paddle. *Nanotechnology* **2010,** *21* (18), 185705.

31.     Ortega, J. M.; Glotin, F.; Prazeres, R., Extension in far-infrared of the CLIO free-electron laser. *Infrared Physics & Technology* **2006,** *49* (1), 133-138.

32.     Dazzi, A.; Glotin, F.; Carminati, R., Theory of infrared nanospectroscopy by photothermal induced resonance. *Journal of Applied Physics* **2010,** *107* (12), 124519.